

VISION BASED OBSTACLE AVOIDANCE AND ODOMETRY FOR SWARMS OF SMALL SIZE ROBOTS

M. Shuja Ahmed, Reza Saatchi and Fabio Caparrelli

Material and Engineering Research Institute, Sheffield Hallam University, Sheffield, U.K.

Keywords: Obstacle Avoidance, Visual Odometry, Swarm Robotics.

Abstract: In multi-robotic systems, an approach to the coordination of multiple robots with each other is called swarm robotics. In swarm robotic systems, small size robots with limited memory and processing resources are used. Integration of vision sensors in such robots can complicate the design of the robots but at the same time, a single vision sensor can be used for multiple objectives as it provide rich surrounding information. As the vision algorithms are normally computationally demanding and robots in swarm systems has limited memory and processing capabilities, so the requirements of light weight vision algorithms also arises. In this research, the use of vision sensor information is made for achieving multiple objectives. A solution to obstacle avoidance, which is the basic requirement as robots move in a cluttered environment and also odometry which is essential for robot localization, is provided using only visual clues. The approach developed in this research is computationally less expensive and suitable for small size robots, where processing and memory constraints limit the use of computationally expensive approaches. To achieve this a library of vision algorithms is developed and customized for Blackfin processor based robotic systems.

1 INTRODUCTION

Current research in the field of swarm robotics is largely focused on providing a computer vision solution to guide multiple robots. In most cases small size robots with limited processing and memory resources, are used. Integration of vision sensor technology in such systems helps to increase the onboard intelligence but at a cost of a significant increase in computational load. The fact that computer vision solutions are computationally very heavy for small size robots, makes collective achievement of tasks challenging among swarm of robots. In this research, a swarm robotic system is considered (shown in figure 1) in which multiple robotic organisms have the ability to physically dock, share information, energy and computational resources with each other and also can locate the charging points to charge their batteries (Kernbach et al., 2010). These swarms of robots can self assemble and can artificially create a single three dimensional robotic organism, which requires these robots to interact with the environment and also with each other. These swarms of robots are expected to perform many different operations in parallel (e.g. docking, communication, scene understanding). Hence, providing vision based senses for guid-

ance and decision making in such robots, naturally requires the development of an efficient and optimized library of vision processing algorithms. This, in turn, helps to achieve real time performance on small size robots. The fact that a vision sensor provides a rich surrounding information (i.e. a single sensor information can be used for multiple purposes), therefore in this research, this visual information is utilized to perform multiple tasks that is, obstacle avoidance and odometry which essentially will help to guide and localize swarm of robots in a structured environment.

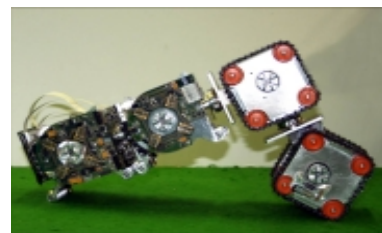


Figure 1: Swarm of robots working collectively (Kernbach et al., 2010).

For autonomous mobile robotic systems, computer vision provides many solutions to obstacle avoidance but when it comes to small size robots, which are also expected to perform many other oper-

ations in parallel, then the number of obstacle avoidance approaches in hand is limited. In (Michels et al., 2005) an obstacle avoidance technique using a monocular vision camera together with a laser range finder is addressed. The testing of the algorithm is performed in a outdoors highly unstructured environment but the testing system used is not strictly an embedded system as all the image processing is done on a development platform so the chances of techniques not meeting the real time constraints were also possible. Another common approach, addressed in (Chao et al., 1999) (Borenstein and Koren, 1985) (Borenstein and Koren, 1988), is based on edge detection. In this method, the algorithm determines the vertical edges of the obstacle and helps robots to move around the edges without colliding against the obstacles. In (Pratt, 2007), the Lucas-Kanade optical flow based algorithm is used for MAVs (Micro Aerial Vehicles) in urban environment. Similarly, in (Souhila and Karim., 2007) Horn and Schunck's optical flow based algorithm is used in autonomous robots. Using optical flow, image velocity vectors are determined which can be split into translational and rotational components. From the translational component, the time to contact information for the obstacle can be calculated which helps in taking necessary actions. Another area of research in computer vision and robotics targeted in this study is the development of efficient visual odometry algorithm for small size robots. In (Maimone et al., 2007), a feature tracking based motion estimation approach is presented to obtain visual odometry information using stereo images captured from NASA's Mars Exploration Rovers (MERs) in a highly unstructured environment. In (Campbell et al., 2005), visual odometry results using optical flow information are presented when the ground robot is moved on a varying terrain including indoor and outdoor environments. The errors reported were 3.3% and 7.1% when the robot is moved on a carpet (high friction) and polished concrete, respectively. Similarly, in (Milford and Wyeth, 2008) (Kyprou, 2009) a scanline intensity based simple algorithm to obtain visual odometry is presented. The odometry error with this algorithm can be large but, in spite of this, notable results are achieved when the odometry information is used with a SLAM (Simultaneous Localization and Mapping) system. A relevant research done in (Schaerer, 2006) addresses the use of line features tracking. Using Hough Transform lines are tracked for obtaining the distance and orientation information. Another algorithm presented in (Younse and Burks, 2007) is based on feature tracking using the Lucas-Kanade algorithm. It also utilizes the information obtained from camera modelling (intrinsic and extrin-

sic parameters) to precisely locate the new position of the vehicle. The average translation error reported when the vehicle moved 30 cm is 4.8 cm and the average rotation errors were 1 and 8 degrees for a 45 and 180 degrees rotation, respectively. This approach performed poorly at high rotation rate as features could move out of the search window. Hence, in the field of autonomous robotics, many approaches to visual odometry (Maimone et al., 2007) (Nistar et al., 2006) (Howard, 2008) using high speed systems are addressed and notable results are achieved. The high computational cost of these algorithms makes them unsuitable for swarms of small size robots. However, further advances in research to provide fast and reactive solutions to these problems is still required. In the following sections, the methods used to perform vision based obstacle avoidance and odometry are detailed in section 2. In section 3, the results obtained when the experiments performed in the in-door environment, are presented. Conclusions are drawn in section 4.

2 METHODOLOGY

The hardware is an important factor which strongly influences the methods adapted to solve the problem at hand. The onboard processing on the robot (shown in Figure 1) was achieved using a high performance 16/32-bit Blackfin BF537E processor. uClinux (micro controller linux), which is a powerful operating system customized for embedded systems, was used as the onboard operating system. Code compilation was done using GNU cross compilers on a Linux based development platform. For the testing and demonstration of the developed vision algorithms, SRV robot by Surveyor Corporation was used. Before proceeding to the complex vision algorithms such as obstacle avoidance and visual odometry, a library of basic vision algorithms was developed. This library was optimised especially for the Blackfin processor architecture. It includes image conversion to different formats (such as YUV to colour image), colour to greyscale image, image gradient using Sobel and Canny operator, region growing based image segmentation, colour blob detection, feature detection using Harris algorithm, cross-correlation based algorithm to solve the feature correspondence problem, image erosion and dilation algorithms. It was decided to add more algorithms as the need arises. In the following sections, the approaches used to perform vision based obstacle avoidance and range of visual odometry algorithms developed are discussed in detail.

2.1 Obstacle Avoidance

There are many ways to accomplish obstacle avoidance but efforts are being made to come up with an algorithm with less computational complexity. For example, algorithms with more floating point operations have more computational complexity and execution time. The Blackfin processor used here is a fixed point processor and can not perform floating point operations efficiently so algorithms with less floating point operations are preferred. Finally, the algorithms are customized to exploit the fixed point Blackfin architecture as suggested in (Lukasiak et al., 2005). Two obstacle avoidance algorithms, where one was based on segmentation and the other utilized the optical flow information, are presented.

2.1.1 Segmentation based Obstacle Avoidance

To explain the concept of segmentation based obstacle avoidance, we considered the image in Figure 2 showing a couple of obstacles. Some assumptions were made that the robot is placed on a flat ground with camera slightly tilted down. In Figure 2b, segmentation result is shown. To determine ground region, one assumption can be that the biggest segmented region is from ground but it may be false when the robot is in front of a big obstacle which result the biggest region. In the current implementation, the speed of the robot is set to guarantee that it is not very close to the obstacle and the region covering the middle bottom of the image is considered to be the ground region. Sometimes, while turning, there is a possibility that the obstacle is very close to the robot. In this scenario, the robot can collide with it. To overcome this problem, the robot keeps track of the intensity of ground region in the last few frames. A sudden change in the intensity helps robot to determines the presence of an obstacle. Following this approach, the isolated ground region is shown in Figure 2c (Total Ground Map). To determine the ground map visible to the robot, the 'Total Ground Map' is filled vertically up with white pixels until the obstacle boundary is detected and the rest of the pixels to the top are filled with black pixels. The same is done for all the columns. The image is finally dilated for refinement. The final visible ground map is shown in Figure 2d. To determine the presence of an obstacle, if from the centre bottom of the final ground map, the number of white pixels are greater than 30 in the vertical direction, then the robot goes straight. It also checks for enough space from left and right direction. If white pixels are less than 30, then the algorithm checks from which side it has more clearance and turn the robot in that direction. In Figure 2d an expected robot trajectory is shown.

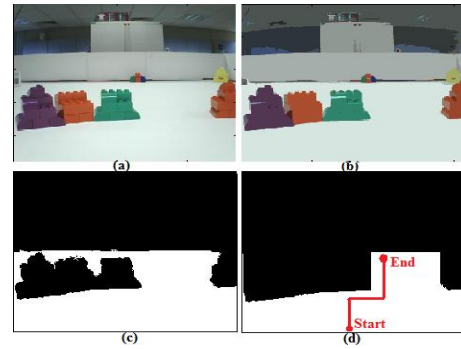


Figure 2: The step by step processing of segmentation based obstacle avoidance algorithm.

2.1.2 Optical Flow based Obstacle Avoidance

Another approach to obstacle avoidance is based on Horn and Schunck (Horn et al., 1993) optical flow information and is inspired from the work done in (Souhila and Karim., 2007). Horn and Schunck derived equations that relate image brightness at a point to the motion of brightness pattern. For this purpose, partial derivatives of the image brightness in x (E_x), y (E_y) directions and in time space (E_t) are obtained. These partial derivatives are used to obtain optical flow vectors u and v in x and y direction, respectively. These vectors are obtained using the following recursive equations.

$$u^{n+1} = \bar{u}^n - \frac{E_x[E_x\bar{u}^n + E_y\bar{v}^n + E_t]}{\alpha^2 + E_x^2 + E_y^2} \quad (1)$$

$$v^{n+1} = \bar{v}^n - \frac{E_y[E_x\bar{u}^n + E_y\bar{v}^n + E_t]}{\alpha^2 + E_x^2 + E_y^2} \quad (2)$$

Where α is a weighting factor and \bar{u}^n and \bar{v}^n are local averages. These recursive equations performs many floating point operations and it was possible to process only one frame in 2 seconds. For faster execution, part of algorithm was coded to perform decimal operations. For this purpose, the necessary precision was determined. For example, for a number 1.3678987, to keep precision upto four decimal point, the number will be multiplied with 10^4 and rest of computation will be done in decimal point format. Where decimal format did not work, fixed point implementation was adopted. This made it possible to process 3.5 frames per second. Now to determine the presence of the obstacle, the image was divided into left and right parts and every time the magnitudes of the optical flow vectors were calculated for these parts. If the sum of these magnitudes exceeds some predefined thresholds, it was assumed that the obstacle is in front of the robot and it turns in the di-

rection which produces less magnitude of the optical flow vectors (i.e. more clearance).

2.2 Visual Odometry

Different approaches to perform visual odometry were implemented and compared with each other. Initially an algorithm, using scan line intensity profile formed by sub images, for obtaining the visual odometry information, was adapted. This scanline profile idea was also adapted in (Pomerleau, 1997) for developing visual steering system and it can also be found in (Milford and Wyeth, 2008) where visual odometry based on single camera was used for SLAM system. The scan line profile is a one-dimensional vector obtained by summing the intensity values in each pixel column of the selected part of the image and then normalized. This vector profile is compared with the other profiles obtained from the consecutive images to extract the rotation and forward distance covered information. Figure 3 shows the top and bottom window images which are used to determine rotation and forward speed, respectively. The scanline idea for obtaining the speed was found very sensitive to lighting conditions and was discarded. So, to obtain the distance covered information, two approaches were examined, i.e. the feature tracking using Lucas-Kanade (Lucas and Kanade, 1981) and feature matching using Normalized Cross Correlation (Lewis, 1995) algorithm. These are explained below.

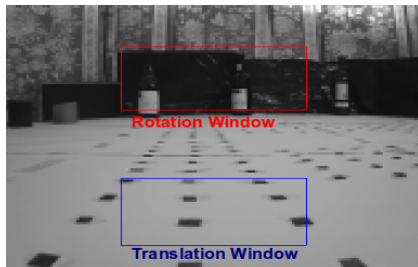


Figure 3: Image parts for rotation and translation cues.

2.2.1 Rotation Estimation

Rotation information is obtained by comparing the scan line intensity profile vectors from two consecutive images captured by the vision system. In Figure 4b, the scan line intensity profiles from two consecutive images are shown. For comparison between the profiles, the average absolute intensity difference $f(t)$ was calculated between the two scanline vectors while a relative shift of the vectors with respect to each other is also performed. The following equation

is used to achieve this task.

$$f(t, V^j, V^k) = \frac{1}{w - |t|} \left(\sum_{n=1}^{w-|t|} |V_{n+\max(t,0)}^j - V_{n-\min(t,0)}^k| \right) \quad (3)$$

where V^j and V^k are the intensity profile vectors to be compared (shown in red and blue colours, respectively, in Figure 4b), t is the amount of pixel shift performed between the two profiles, and w is the width of the windowed image. In Figure 4a, the absolute intensity differences graph, when one profile vector is shifted over the other, is shown. The pixels shift p_s were obtained by determining the value t which minimizes the function $f(t)$ for the vectors V^j and V^k :

$$p_s = \min_{t \in [\rho-w, w-\rho]} f(t, V^j, V^k) \quad (4)$$

The selection of offset ρ was made such that there was enough overlap between the two profiles. The values used for w and ρ were 88 and 40, respectively. For the two profiles shown in Figure 4b, the value of pixel shift p_s obtained is 15 pixels in the left direction from the center of image. This pixel shift is multiplied by gain factor α to perform conversion into an angular shift value $\Delta\theta$. The value of α can be obtained empirically or by using the camera's intrinsic parameters:

$$\Delta\theta = \alpha p_s \quad (5)$$

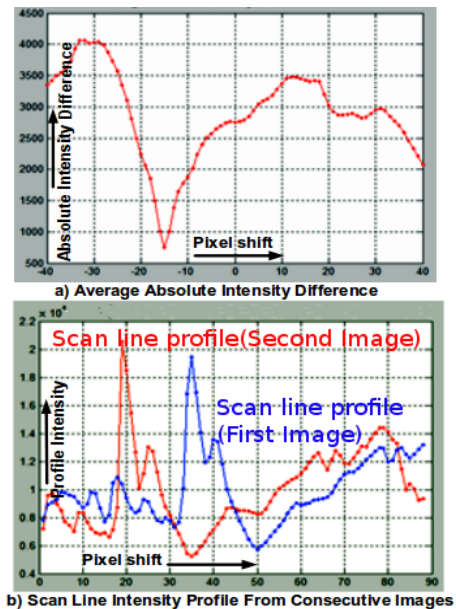


Figure 4: a) Average intensity difference when one profile shifted over the second. b) Two scanline profiles.

2.2.2 Translation Estimation using Lucas-Kanade Feature Tracking

The translation estimation algorithm is divided into two tasks. The first is to detect salient features in the image and the second is the features tracking. For feature detection, Harris feature detection (Harris and Stephens, 1988) algorithm was implemented. The features detected were then tracked in the following images by the Lucas-Kanade tracking algorithm. The basic idea of the Lucas-Kanade (Lucas and Kanade, 1981) tracking algorithm is the following. Let, I_1 and I_2 be two images and u be a feature detected on image I_1 , where $u = [x, y]$ and $I_1(u) = I_1(x, y)$. Then, the goal of the Lucas-Kanade tracking is to find the location $v = u + d$ on the second image I_2 such that $I_1(u)$ and $I_2(v)$ are similar. Let, d be the image velocity vector at point u . The next step is to define a neighbourhood around feature u (i.e. w_x and w_y in x and y directions), where similarity analysis between u and v can be made. Then, vector d can be defined as the one which minimizes the following residual function:

$$\epsilon(d) = \sum_{x=u_x-w_x}^{u_x+w_x} \sum_{y=u_y-w_y}^{u_y+w_y} [I_1(x, y) - I_2(x+d_x, y+d_y)]^2 \quad (6)$$

After obtaining the velocity vector, the new feature location can be determined and tracked. For odometry, the average shift made by the feature in y direction (after multiplying by scale factor) is used to determine the translation and the shift in x direction is used for the small rotation information. To measure large rotation, scan line algorithm is used in parallel.

2.2.3 Translation Estimation using Normalised Cross Correlation Feature Matching

Another approach developed in this work was based on Normalised Cross Correlation matching of salient features. The features are detected in two images using the Harris algorithm. Matching and correspondence between the features is performed using normalised cross correlation algorithm. In this algorithm, to perform feature matching, a small template is taken around each feature in one image and is matched with the other image within a predefined search window. The basic equation used to perform cross correlation matching is given below.

$$C(m, n) = \frac{\sum_{x,y} [I(x, y) - \bar{I}_{m,n}] [t(x-m, y-n) - \bar{t}]}{[\sum_{x,y} [I(x, y) - \bar{I}_{m,n}]^2 \sum_{x,y} [t(x-m, y-n) - \bar{t}]^2]^{0.5}} \quad (7)$$

In this equation, $I(x, y)$ is the image and $t(x, y)$ is the target template (i.e. template around feature), \bar{t} is the

mean of the template and $\bar{I}_{m,n}$ is the mean of the image. Once corresponding features are identified, then the average pixel shift in x and y direction is used to determine the rotation and translation, respectively. For large rotation, scan line works in parallel.

3 RESULTS

This section is dedicated to the results. It includes obstacle avoidance using segmentation/optical flow information and visual odometry results from scan line based rotation, Lucas-Kanade tracking and normalised cross correlation based translation algorithm.

3.1 Obstacle Avoidance

To test this algorithm, a test platform was developed. Obstacles were placed on uniform white surface. Some processed images are shown in Figure 5. When the algorithm finds that the white pixels to the obstacle boundary are less than 30, then it determines which side gives more clearance and turns in that direction. Factor 30 pixels is determined empirically.

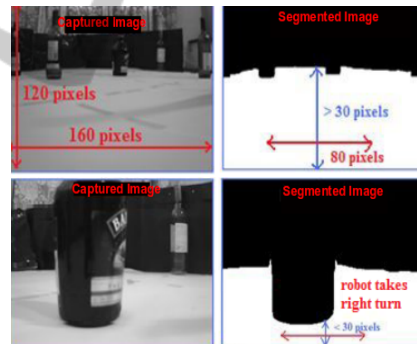


Figure 5: Segmentation based obstacle avoidance.

Using this algorithm, many tests were performed. One of the path followed by the robot is shown in Figure 6a. The maximum frame rate achieved with this approach is 2.46 frames per second.

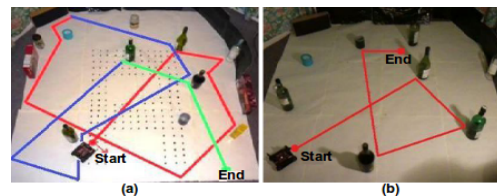


Figure 6: (a) Segmentation result (b) Optical flow result.

A trajectory made by the robot using optical flow

algorithm, is shown in Figure 6b. In Figure 7, the optical flow information generated from the two consecutive images, when the robot was moving in forward direction, is shown. A zoomed-in version of the optical flow field is also shown. The optical flow vectors obtained are in the correct direction (i.e. opposite to the direction of motion) but there are some vectors in random directions and act as noise. The maximum frame rate achieved with this approach is 3.5 frames per second.

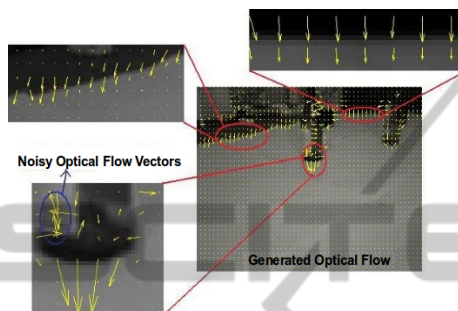


Figure 7: Optical flow field between 2 consecutive images.

3.2 Visual Odometry

For visual odometry, the scanline algorithm was used for getting the rotation estimates. In Figure 8, the results obtained, when the robot was making a square trajectory, are shown. The robot moved equal distances after every 90 degrees turn. In Figure 8a, the angle measurement obtained from the visual odometry is shown. Robot has taken 89.5, 92, 91 and 88 degrees turns in place of 90 degrees turn. The resultant square trajectory is also shown in Figure 8b. This rotation and translation measurements are obtained using the scanline profile based algorithm. The scanline algorithm for translation is found very sensitive to the lighting conditions. It gives totally different translation estimates in a different environment. So here, accuracy achieved in rotation using scanline is focused.

To obtain the accuracy in translation estimates, the feature based approach was used. For features detection, black marks were made on the ground surface. In Figure 9, some of the results obtained from the Lucas-Kanade tracking (left column) and feature matching results from the normalised cross correlation algorithm (right column) are shown.

To test feature based translation estimation algorithm, two tests were performed. In Figure 10a, the visual odometry results obtained from test 1, when the robot was moved 36 inches forward, took a 90 degree right turn and then moved 11 inches, are shown. In the results obtained from the Lucas-Kanade algorithm, the robot moved 38.6 inches forward and 10

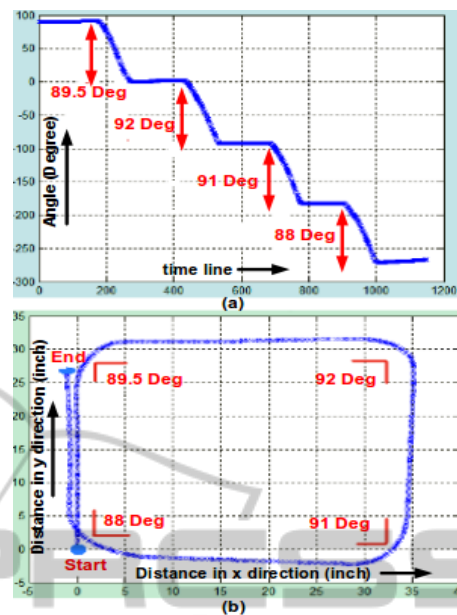


Figure 8: Angle information and the actual trajectory obtained from visual odometry for square trajectory.

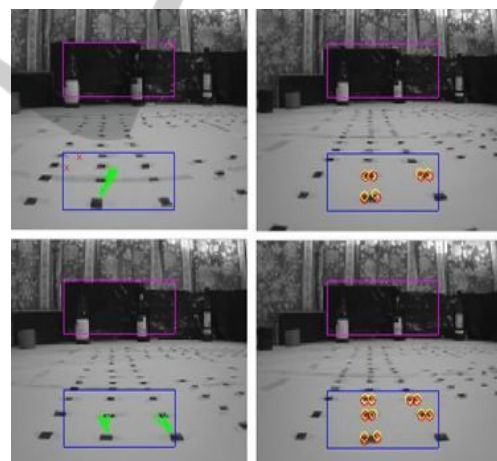


Figure 9: Lucas-Kanade and Normalised cross correlation feature tracking and matching results.

inches after taking a right turn. According to the measurements obtained using the cross correlation based algorithm, the robot moved 38.7 inches forward and then 9.5 inches after taking a right turn. Both of these measurements are very close to the actual trajectory made by the robot. Similarly, Figure 10b shows the results obtained from test 2 when the robot moved 36 inches forward, took a 90 degree left turn and then moved 9.5 inches. According to the measurements obtained using the Lucas-Kanade algorithm, the robot moved 37.4 inches forward and 8.3 inches after taking a left turn. According to the cross correlation based

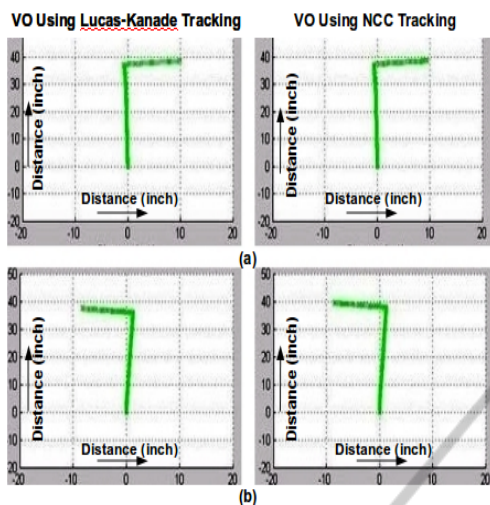


Figure 10: Visual odometry (a) test 1 (b) test 2.

algorithm, the robot moved 39.4 inches forward and 8.6 inches after taking a left turn.

4 CONCLUSIONS

In this research, vision algorithms for a Blackfin based small size robotic system have been developed. For obstacle avoidance, a slightly slower frame rate was achieved but it can be improved by implementing the computationally expensive sections of the code in assembly language. For visual odometry, the Lucas-Kanade based approach has provided good results when tested using Matlab. But it is found that, in case of features lost, some time it provides less accuracy than expected. It is concluded that, the use of scan line based rotation information with the feature based approach provide an efficient solution to visual odometry but at the same time, it can be easily deceived if the robot come close to a moving object such as another robot. To overcome this, information from visual odometry may be fused together with the wheel odometry to determine whether the robot was actually moved or object in the environment moved.

ACKNOWLEDGEMENTS

This research was funded by European Commission Seventh Framework Programme FP7/2007-2013 research project REPLICATOR.

REFERENCES

- Borenstein, J. and Koren, Y. (1985). A mobile platform for nursing robots. In *IEEE Transactions on Industrial Electronics*, Vol. 32, No. 2.
- Borenstein, J. and Koren, Y. (1988). Obstacle avoidance with ultrasonic sensors. In *IEEE journal of robotics and automation*, vol. ra-4, no. 2.
- Campbell, J., Sukthankar, R., Nourbakhsh, I., and Pahwa, A. (2005). A robust visual odometry and precipice detection system using consumer-grade monocular vision. In *Proc. ICRA, Barcelona, Spain*.
- Chao, M., Braunl, T., and Zaknich, A. (1999). Visually-guided obstacle avoidance. In *6th International Conference on Neural Information Processing ICONIP*.
- Harris, C. and Stephens, M. (1988). A combined corner and edge detector. In *Proceedings of the 4th ALVEY vision conference, University of Manchester, England*.
- Horn, Berthold, K. P., and Schunck, B. G. (1993). Determining optical flow. In *Artificial Intelligence: 81-87*.
- Howard, A. (2008). Real-time stereo visual odometry for autonomous ground vehicles. In *IEEE/RSJ International Conference on Intelligent Robots and Systems*.
- Kernbach, S., Scholz, O., Harada, K., Popescu, S., Liedke, J., Raja, H., Liu, W., Caparrelli, F., Jemai, J., Havlik, J., Meister, E., and Levi, P. (2010). Multi-robot organisms: State of the art. In *ICRA 2010 Workshop Modular Robots: State of the Art*.
- Kyprou, S. (2009). Simple but effective personal localisation using computer vision. In *MEng Report. Department of Computing, Imperial College London*.
- Lewis, J. P. (1995). Fast template matching. In *Vision Interface*, p. 120-123.
- Lucas, B. D. and Kanade, T. (1981). An iterative image registration technique with an application to stereo vision. In *IJCAI*.
- Lukasiak, R., Katz, D., and Lukasiak, T. (2005). Enhance processor performance in open-source applications. In *Analog Dialogue 39-02*.
- Maimone, M., Cheng, Y., and Matthies, L. (2007). Two years of visual odometry on the mars exploration rovers. In *Journal of Field Robotics. Special Issue: Special Issue on Space Robotics. Volume 24, Issue 3*.
- Michels, J., Saxena, A., and Andrew, Y. (2005). High speed obstacle avoidance using monocular vision and reinforcement learning. In *Proceedings of the 22nd International Conference on Machine Learning*.
- Milford, M. and Wyeth, G. (2008). Mapping a suburb with a single camera using a biologically inspired slam system. In *Robotics, IEEE Transactions on*, vol.24, no.5, pp.1038-1053, Oct. 2008.
- Nistar, D., Naroditsky, O., and Bergen, J. (2006). Visual odometry for ground vehicle applications. In *Journal of Field Robotics, Volume 23*.
- Pomerleau, D. (1997). Visibility estimation from a moving vehicle using the ralph vision system. In *IEEE Conf. Intelligent Transportation Systems*.
- Pratt, K. (2007). Smart sensors for optic flow, obstacle avoidance for mavs in urban environments. In *International Journal of Advanced Robotic Systems*.

- Schaerer, S. S. (2006). Practical visual odometry for small embedded systems. In *Master's Thesis, Department of Electrical and Computer Engineering, University of Manitoba*.
- Souhila, K. and Karim., A. (2007). Optical flow based robot obstacle avoidance. In *International Journal of Advanced Robotic Systems*.
- Younse, P. J. and Burks, T. F. (2007). Greenhouse robot navigation using klt feature tracking for visual odometry. In *International Commission of Agricultural Engineering. CIGR E-Journal Volume 9*.

